ELSEVIER

Chemical Engineering Journal 91 (2003) 219–225

Chemical Engineering Journal

www.elsevier.com/locate/cej

Motion of particles through the fixed bed in a gas–solid–solid downflow reactor

L.V. Barysheva*, E.S. Borisova, V.M. Khanaev, V.A. Kuzmin, I.A. Zolotarskii, N.A. Pakhomov, A.S. Noskov

Boreskov Institute of Catalysis, Pr. Akademika Lavrentieva 5, 630090 Novosibirsk, Russia

Abstract

The experimental studies and mathematical modeling are presented for the residence time distribution of fine solids moving in a co-current downflow fixed-bed reactor. Experiments were carried at ambient conditions using a glass column of 30 mm i.d. packed by spheres of 4–6 mm diameter. Fine alumina of 50–250 μm was used as a moving solids. Solids flow rate was varied from 0.1 to 0.5 g cm^{-2} s^{-1}. The new flight-time technique is applied to measure residence time of fine particles in a packed bed. The influence of particle size and flow rate on the particles residence time is experimentally investigated. New three-dimensional model of moving of fine particles in a packed bed is developed. The model is based on the statistical calculations of an individual particle path in a packed column. Model validation was checked by comparing experimental values of particles residence time distribution with calculated one. Calculated values of particles residence time were found to be in a good agreement with experimental data at the solids flow rate below 0.1 g cm^{-2} s^{-1}.

Keywords: Gas–solid–solid reactor; Fixed bed; Gas–solid co-current downflow; Residence time distribution

1. Introduction

Usage of moving solid particles as a heat carrier in a fixed catalyst bed reactors seems to have definite advantages for highly endo- and exothermic processes, because moving particles provides additional heat supply to the reaction zone. Moreover, moving particles have strong influence on the rate of heat and mass transfer in a catalyst bed. Rate of mass transfer between catalyst and gas–solid flow depends on the velocity of moving particles. Rate of heat transfer between gas (U_g) and moving particles (U_s) depends on the relative particles velocity

$$U_r = U_g - U_s$$

Interstitial gas velocity U_g, in turn, depends on a part of free volume ε_s occupied by moving solids

$$\varepsilon_s = 1 - \frac{G_s}{\rho_s \varepsilon U_s}$$

So, particles velocity and particles residence time are key parameters for reliable estimations of heat and mass transfer coefficients in a gas–solid–solid reactor.

Generally, cold flow studies are used to investigate basis of hydrodynamics of fluidized and fixed-bed reactors. Fundamental studies of the hydrodynamics of countercurrent trickle flow of particles are reported in literature [1,2]. Hydrodynamics of a gas–solid–solid circulating fluidized bed reactor was also studied [3]. However, in spite of co-current downward fixed-bed reactors have definite advantages in comparison with countercurrent flow reactors, only scarce data concerning the hydrodynamics of co-current downward fixed-bed reactors are available. Compared with upflow reactor, the downflow reactor diminishes axial dispersion of solid particles resulting to a narrow residence time distribution of gas and solid particles. Another advantage of co-current downward reactor is their ability to be operated at wider range of gas velocity in comparison with countercurrent reactor.

Modeling of gas and solids flow through a fixed bed has been started recently. By the moment there are three distinct branches of modeling of solids flow in a packed bed: (1) modeling of formation of packed bed [4]; (2) description of moving particle interactions with a reactor walls [5]; and (3) network models [6,7]. It seems to be interesting to combine these branches in the single mathematical model of gas–solid–solid reactor for providing more accurate description of particle flow through the fixed bed.

* Corresponding author. Tel.: +7-3832-341878; fax: +7-3832-341878.
E-mail address: barysheva@catalysis.nsk.su (L.V. Barysheva).

1385-8947/02/$ – see front matter © 2002 Elsevier Science B.V. All rights reserved.
PII: S1385-8947(02)00157-2

Nomenclature

d	diameter of particles (m)
D	diameter of packing particles (m)
g	gravitational acceleration ($m\,s^{-2}$)
G_s	solids flow rate ($g\,cm^{-2}\,s^{-1}$)
k	measurement channel number
k_t	friction coefficient
K	restitution coefficient of solids with packing particle or wall
L	bed height (m)
m	particle mass (kg)
n	the number of measurement points
N	supporting force ($kg\,m\,s^{-2}$)
$\vec{R}$	radius vector of moving particle (m)
Re	Reynolds number defined by $\rho_g d U_r/\mu_g$
S_k	signal level of the corresponding channel
S_{k0}	zero signal level
S_m	particle midship (m^2)
t	time (s)
ΔT	average time of particles residence in the fixed bed (s)
$\vec{U}_g$	gas superficial velocity ($m\,s^{-1}$)
U_n	normal component of velocity ($m\,s^{-1}$)
U_s	average velocity of resident particles in the fixed bed ($cm\,s^{-1}$)
U_t	tangential component of velocity ($m\,s^{-1}$)
$\vec{U}_p$	particle velocity vector ($m\,s^{-1}$)
V	particle volume (m^3)

Greek symbols

ε	porosity
ε_s	part of free volume occupied by moving solids
$\zeta\ (Re)$	particles aerodynamic resistance coefficient defined by $\varsigma(Re) = 24/Re(1 + 0.158Re^{2/3})$
θ, φ, R	spatial spherical coordinates
ρ	particle density ($kg\,m^{-3}$)
ρ_g	gas density ($kg\,m^{-3}$)
τ	quantization time (s)

Main purpose of the present paper was

(1) to measure particles residence time in a gas–solid–solid downflow reactor by applying new experimental technique;
(2) to present new model of particles moving through the packed bed model and to simulate residence time distribution of particles;
(3) to check model validation by comparing of calculated particles residence time and measured one.

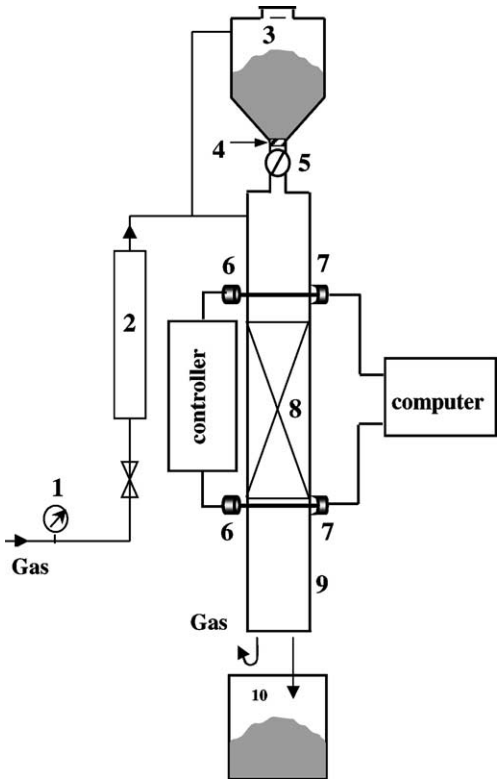

Fig. 1. Schematic of experimental set-up; 1: pressure gauge; 2: rotameter; 3: vessel; 4: plate with calibrated holes; 5: flow governor; 6: light-emitting diodes; 7: photodetectors; 8: packed bed; 9: glass column; 10: reservoir.

2. Experimental set-up and procedures

2.1. Experimental installation

Experiments were carried out at 1 atm and ambient temperature. The experimental installation is shown schematically in Fig. 1. It is consisted of a glass tube of 30 mm internal diameter packed by spherical particles of 4–6 mm diameter. Spheres were arranged in the column in an irregular manner. Installed at the tube bottom was the grid to support bed packing. The grid did not affect fine particles flow due to having large free section. Fine solids and gas were fed at the column top. So, gas and solids moved from the bed top to the bottom in a co-current flow. At the tube bottom gas was released to the atmosphere and particles were accumulated in a reservoir.

Solids were supplied to the tube from a vessel through the plate having calibrated holes. Solids flow rate was varied from 0.125 to 0.5 $g\,cm^{-2}\,s^{-1}$ by changing holes size.

2.2. Special equipment

A flight-time technique was used for experimental measurements of residence time of particles moving through the packed bed. The particles residence time in the bed was measured using specific devices, including two light-emitting

diodes and two photodetectors. Upper light-emitting diode and photodetector were installed at the bed top, and another light-emitting diode and photodetector were installed at the bed bottom. The upper light-emitting diode and photodetector were mounted at 2 cm above the bed surface to keep them from particles reflected from the bed. Photodetectors measure the intensity of light emitted by diodes. When solids cross the light beam, intensity of photodetector signal is weakened due to partial screening of the light by particles. The light signal intensity is in inverse proportion to the number of particles in the light beam. Output signal from photodetector was recorded by analog-to-digital converter (ADC) at the frequency of 4 and 10 kHz.

2.3. Fines properties

Alumina having bulk density of 1000 kg m^{-3} was used as a moving solids. To investigate the influence of particle size on the particles residence time experiments were carried out using three different sets of particles having different particle size distribution:

(1) 50–150 μm;
(2) 150–180 μm;
(3) 180–250 μm.

2.4. Experimental data processing

Solids were supplied to the bed by small portions. If the volume of single solids portion was large enough (1 ml), signal from the upper photodetector installed at the tube inlet approached to rectangular shape. Signal from lower photodetector was recorded time shifted and looked like a distorted input signal (Fig. 2).

The average particle residence time in the fixed bed was determined as follows:

$$M_{k0} = \sum_{i=1}^{n} (S_{k,i} - S_{k0}), \quad k = 1, 2 \tag{1}$$

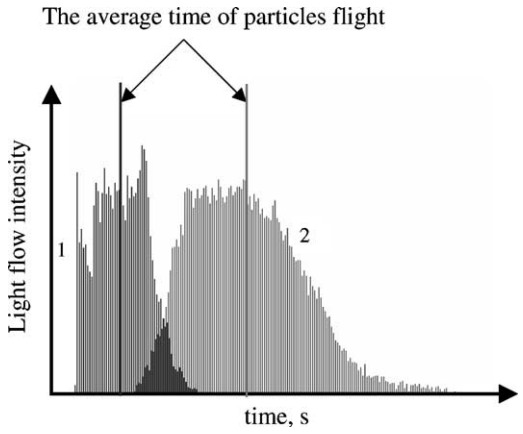

Fig. 2. Recorded signal from photodetector; 1: input signal; 2: output signal.

$$M_{k1} = \sum_{i=1}^{n} \tau i (S_{k,i} - S_{k0}), \quad k = 1, 2 \tag{2}$$

The average residence time ΔT and average particle velocity U_s were calculated as follows:

$$\Delta T = \frac{M_{21}}{M_{20}} - \frac{M_{11}}{M_{10}} \tag{3}$$

$$U_s = \frac{L}{\Delta T} \tag{4}$$

Experimental quantization time (τ) was chosen equal to 100 and 250 μs. The ΔT was found to be independent on the quantization time.

3. Model development

Mathematical modeling of particles flow through a packed bed was performed at two stages. First, computer simulation of packed bed formation was performed and then calculations of particle motion through the fixed bed were carried out.

3.1. Simulation of packed bed formation

Algorithms of bed formation could be found elsewhere [4]. A new program for generation of the structure of a packed bed was developed. Program for bed generation has the following assumptions:

(1) bed is packed by spheres having an equal size;
(2) bed starts packing from the bottom;
(3) the first bed layer is randomly arranged (the ordered packing is a particular case);
(4) next spheres occupy steady positions with three points of support (three spheres or two spheres and the wall). Thus stacked spheres build up the final array of potential sites for the next layer of spheres. These potential sites may be competitive vacancies, i.e. they are unrealizable simultaneously but chosen according to the packing algorithm.

A distinctive feature of the program was using of different packing modes. Each next particle could placed to (1) site having a minimal potential energy (“deepest” site); (2) random site (by random-number algorithm); (3) site nearest from the reactor wall; and (4) site nearest from the reactor axis.

3.2. Calculation of particles motion through a packed bed

The model was based on the calculations of trajectory of the individual particle moving through the three-dimensional packed bed. Particle motion includes the following components: (1) motion through the inter-sphere space; (2) collisions with spheres or with the reactor walls; (3) sliding over

the sphere surface. To model particle motion the following assumptions were made:

(1) moving particles do not interact with each other;
(2) gravity, aerodynamic resistance, inelastic collisions between particles and spheres, sliding of particles over the sphere surface are key factors determining the motion.

The paths and residence times of individual particles were calculated at different initial coordinates. The average particle residence time in the fixed bed (ΔT) was determined as an arithmetic mean these residence times.

The model can be described by the following equations:

1. Equation of particle motion

$$m\frac{\mathrm{d}\vec{U}_\mathrm{p}}{\mathrm{d}t} = V(\rho - \rho_\mathrm{g})\vec{g} + 0.5\varsigma(Re)S_\mathrm{m}\rho_\mathrm{g}\vec{U}_\mathrm{r}U_\mathrm{r} \quad (5)$$

$$\frac{\mathrm{d}\vec{R}}{\mathrm{d}t} = \vec{U}_\mathrm{p} \quad (6)$$

where $\vec{U}_\mathrm{r} = \vec{U}_\mathrm{g} - \vec{U}_\mathrm{p}$. Initial conditions for each moving particle are: $t = 0$; $\vec{U}_\mathrm{p} = 0$; $z = 0$; x, y coordinates were varied.

Particles are uniformly distributed through level $z = 0$ and start moving at the same time moment at $t = 0$. While moving through the packing bed, the particle can collide with the catalyst granules and with the reactor wall or slide over the surface of the catalyst granule or of the wall.

2. Collision-induced changes in the moving particle velocity are described by the following equations:

$$U_\mathrm{n}^{+} = -KU_\mathrm{n}^{-} \quad (7)$$

$$U_\mathrm{t}^{+} = U_\mathrm{t}^{-} \quad (8)$$

where symbols '+' and '−' are used to indicate *after* and *before* the collision, respectively.

3. Sliding of a particle over the granule surface is described by equations in spherical coordinates with the center coinciding with the center of the granule and with axes directed as shown in the following figure

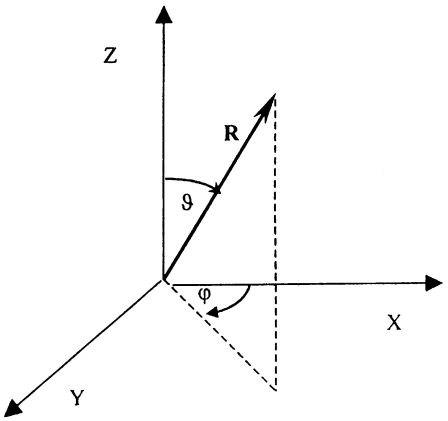

Equations of particle sliding over the sphere surface are

$$\ddot{\theta} - \dot{\varphi}^2 \sin\theta\cos\varphi = \frac{2g\sin\theta}{D+d} - \frac{2k_\mathrm{t}N}{m(D+d)}\frac{U_\theta}{|U|} \quad (9)$$

$$\ddot{\varphi}\sin\theta + 2\dot{\varphi}\dot{\theta}\cos\varphi = -\frac{2k_t N}{m(D+d)}\frac{U_\varphi}{|U|} \quad (10)$$

$$N = -mg\cos\theta + \tfrac{1}{2}m(D+d)(\dot{\theta}^2 + \dot{\varphi}\sin\theta) \quad (11)$$

Similar equations describe the sliding over the reactor wall.

If $U_\mathrm{n} \approx 0$ at the moment of a collision between the particle and the sphere or the reactor wall, the particle is considered to start sliding over the sphere surface, and the motion is described by equation set (Eqs. (9)–(11)). The condition of the particle detachment from the sphere surface is $N = 0$. Eqs. (4) and (5) are used again to describe the particle motion after the detachment.

The collision elasticity is characterized using the restitution coefficient (K) at the particle collision with the packing granules or the reactor walls. $K = V_+/V_-$, where V_+ and V_- are normal components of the velocity before and after the collision, respectively. The restitution coefficient show how the velocity of a small particle changes upon collision with a coarse particle or with the reactor wall. It depends on the material of the colliding bodies. $K = 1$ for the absolutely elastic impact and $K = 0$ for the absolutely inelastic impact. $K = 0.95$ for glass balls and $K = 0.55$ for steel balls [8]. We chose $K = 0.8$ for alumina spheres.

A specific feature of direct mathematical modeling is that this technique requires a bulk computations. The accuracy of these methods usually increases with the number of particles used for the computation, so increasing computation time. Reasonable compromise between the amount of computations and ability to simulate phenomena, which are not treatable by the other numerical methods, can be met using differential schemes of low order of accuracy for approximation of motion equations. In this case, the path of each individual particle is calculated at comparatively low accuracy, but such an approach enables to obtain statistically stable results. In the present work, the differential scheme of the first order was constructed to find coordinates of the particle radius vector; the Runge–Kutta method of the second order was used to determine coordinates of the velocity vector. Basic characteristics of a solid flow constituted by a large number of particles (100,000–1,500,000), which are the average flow rate along the reactor radius and the particle residence time distribution through the bed, are statistically stable. The model will be discussed in more detail in the next paper. $\vec{U}_g = 0$ was assumed for calculations based on experimental observation of no remarkable influence of gas velocity on the particle velocity within the investigated range of parameters (see Fig. 7).

Data calculated with the described model are presented in Fig. 3. Parameters chosen for calculation were $D = 5.2 \times 10^{-3}$ m, $d = 2 \times 10^{-4}$ m, $L = 9 \times 10^{-2}$ m and $K =$

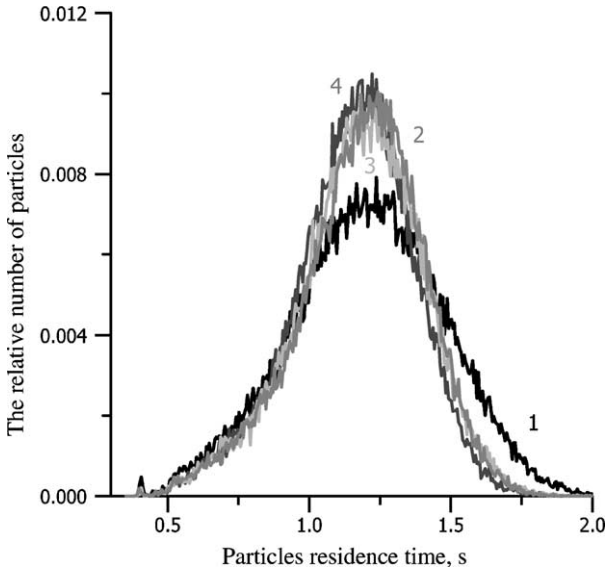

Fig. 3. Effect of packing procedure on the particles residence time; 1: bed is packed according to the minimum potential energy; 2: bed is packed according to the random algorithm; 3: bed is packed from reactor axis; 4: bed is packed from reactor wall.

Table 1
Calculated bed porosity (ε) for different arrangement modes

Number of curve	Packing procedure	ε	Particles residence time (s)
1	Minimum potential energy	0.469	0.897
2	From reactor wall	0.500	0.878
3	From reactor axis	0.508	0.871
4	Random algorithm	0.516	0.851

0.8. The results obtained illustrate the influence of packing procedure on the particle residence time. Table 1 presents calculated bed porosity (ε) for different arrangement modes. The lowest porosity corresponds to the case when each next particle of the bed occupies the minimal potential energy sites. The highest porosity is observed for random packing. Different porosities are characteristic of different arrangements. However, Fig. 3 and calculated data (Table 1) show a weak influence of the bed arrangement on the particle residence time.

4. Results and discussion

Comparison of experimental (curve 2) and calculated (curve 3) data for the case when particles distribution before the beds corresponds curve 1 is given in Fig. 4. All particles fed to the tube move at approximately equal rates until reach the bed. That is why an input signal from upper photodetector (curve 1) has almost rectangular shape. The computed curve was shown to feet well mean experimental signal from lower detector for the flow rate of

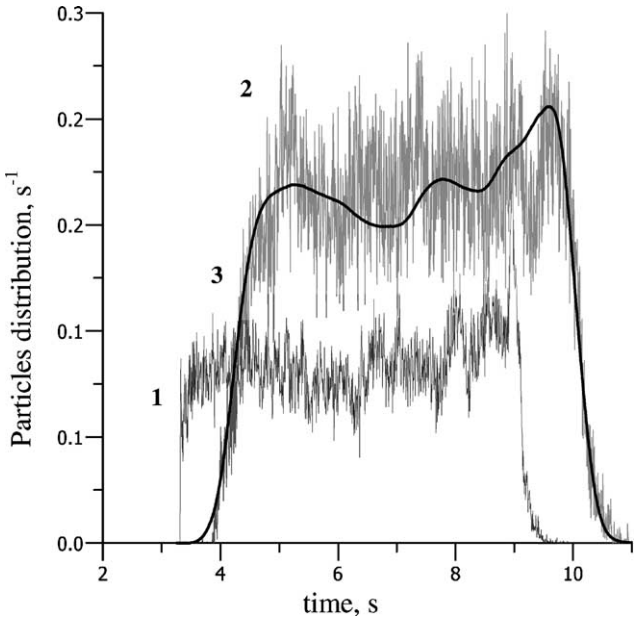

Fig. 4. Time distribution of particles; 1: before the bed in the scale 1:2; 2: after the bed; 3: calculated curve of particles distribution after the bed ($K = 0.8$). The averaging interval is 5×10^{-3} s. Experimental conditions: packed bed—alumina fraction 4–5 mm, height—9 cm; solids—alumina fraction 150–180 μm; $G_s = 0.025\,g\,cm^{-2}\,s^{-1}$.

$0.025\,g\,cm^{-2}\,s^{-1}$. Hence, this is an appropriate model for description of experimental data at low flow rates.

Experimental and calculated data obtained for higher flow rates under otherwise identical conditions (solid and packing fractions) are compared in Fig. 5. Qualitative difference

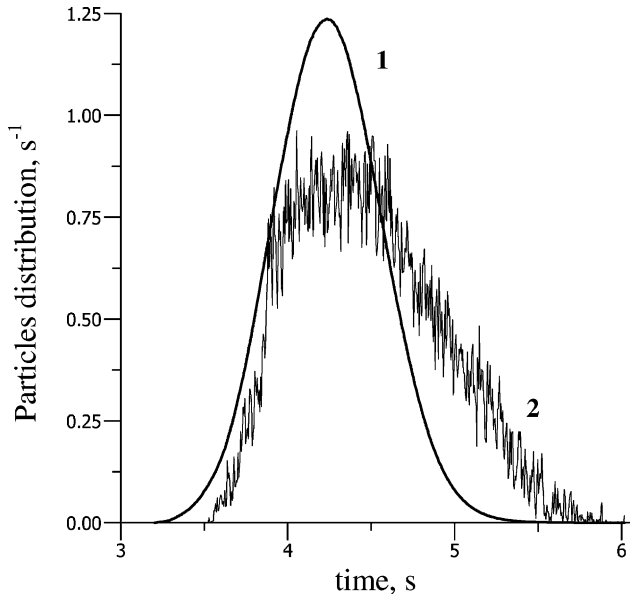

Fig. 5. Time distribution of particles after the bed; 1: calculated curve ($K = 0.8$); 2: experimental curve. The averaging interval is 5×10^{-3} s. Experimental conditions: packed bed—alumina fraction 4–5 mm, height—9 cm; solids—alumina fraction 150–180 μm, $G_s = 0.45\,g\,cm^{-2}\,s^{-1}$.

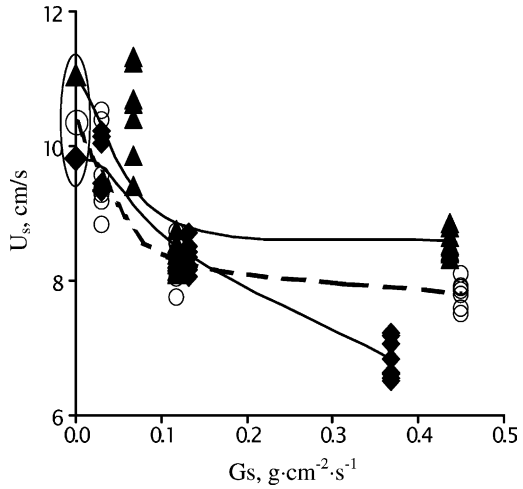

Fig. 6. The effects of the solids flow rate (G_s) on the solid velocity (U_s). Solids fractions are: (▲), 50–150 μm; (○), 150–180 μm; (◆), 180–250 μm. Packed bed—alumina fraction 4–5 mm; height—9 cm. Points on ordinates axis are obtained by a model ($K = 0.8$).

between experimental and calculated curves are shown in the figure. In particular, the calculated curve shows a shorter average time than the experimental curve. This difference appears because the model does not consider the influence of interaction between particles in the flow which becomes noticeable as the flow rate increases. Similar curves were obtained for different solid fractions.

Fig. 6 illustrates the influence of the solids flow rate on the solids velocity experimentally obtained. An increase of solids flow rate results to decreasing of solids velocity due to appearing of essential reciprocal particles interactions. An increase a size of solid particles results in some decrease in their filtration rate. This effect becomes more pronounced as the solids flow rate increases. The solids velocity (U_s) depends only slightly on particles size at $G_s < 0.1\,g\,cm^{-2}\,s^{-1}$ while the dependence is more remarkable at higher G_s. The reason is that motion of a larger particle, unlike the motion of fine particles, through the intergranule voids in the fixed bed is impeded by other moving particles.

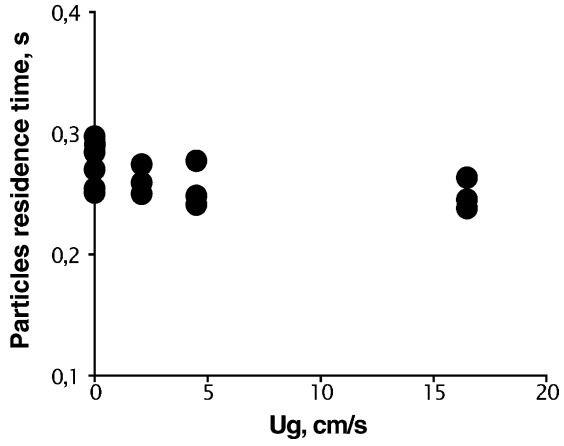

Fig. 7. The effects of gas superficial velocity (U_g) on the particles residence time. Packed bed is porcelain spheres $D = 6$ mm. Solids is alumina fraction 150–180 μm.

Dependence of average solids velocities U_s on solids rate G_s illustrated in Fig. 6. Simulated values of solids velocity U_s are plotted at ordinate axis (i.e. when $G_s = 0$) because the present model does not take into account interparticle interactions that corresponds to very low solids rate. One can see that calculated data are close to the experimental values at the range below $0.1\,g\,cm^{-2}\,s^{-1}$.

An influence of gas velocity on the particles residence time is shown in Fig. 7. Negligible variations in the residence time are observed in the range of gas velocities between 0 and $17\,cm\,s^{-1}$ that agrees with literature data [2].

5. Summary

1. The flight-time technique was proposed for measuring residence time of particles in the packed bed.
2. The influence of gas velocity (in the range from 0 to $17\,cm\,s^{-1}$), size of moving particles (50 to 250 μm) and solids flow rate ($0.125–0.5\,g\,cm^{-2}\,s^{-1}$) on the particles residence time was experimentally determined. The gas velocity was shown not to affect the particles residence time. The influence of the particle size on particles velocity was only observed at the solids flow rate higher than $0.1\,g\,cm^{-2}\,s^{-1}$. The residence time was found to increase on increasing in the solids flow rate and the particle size.
3. A mathematical model was developed for description of particle motion through the fixed bed. The model takes into account the following features:
   - influence of packing procedure;
   - gravity;
   - aerodynamic resistance;
   - inelastic collision between particles and spheres;
   - particle sliding over the sphere surface.

It was shown that the values calculated using the proposed model are in good agreement with experimental data at solids flow rate below $0.1\,g\,cm^{-2}\,s^{-1}$. At a higher flow rate, there is considerable interaction between the particles that falls outside the model.

References

[1] K.R. Westerterp, M. Kuczynski, Gas-solid trickle flow hydrodynamics in a packed column, Chem. Eng. Sci. 42 (1987) 1539–1551.
[2] M. Benaly, K. Shakourzadeh-Bolouri, The gas-solid-solid packed contactor: hydrodynamic behaviour of countercurrent trickle flow of coarse and dense particles with a suspension of fine particles, Int. J. Multiphase Flow 20 (1994) 161–170.
[3] S. Huang, Z. Wang, Y. Jin, Studies on gas-solid-solid circulating fluidized-bed reactors, Chem. Eng. Sci. 54 (1999) 2067–2075.

[4] K. Nandakumar, Y. Shu, K.T. Chuang, Predicting geometrical properties of random packed beds from computer simulation, AIChE J. 45 (1999) 2286–2297.
[5] A.V. Nguyen, C.A.J. Fletcher, Particle interaction with the wall surface in two-phase gas-solid particle flow, Int. J. Multiphase Flow 25 (1999) 139–154.
[6] S.D. Rege, H.S. Folger, A network model for deep bed filtration of solid particles and emulsion drops, AIChE J. 34 (1988) 1761–1772.
[7] K.E. Thompson, H.S. Folger, Modeling flow in disordered packed beds from pore-scale fluid mechanics, AIChE J. 43 (1997) 1377–1389.
[8] H. Ebert, Physikalisches taschenbuch, Braunschweig, 1957.